Instabilities in Two-Phase Flow of Complex Fluids

Authors: Allen Cameron, Xizhi Cao, Antonio Jurko, Lucas Lamb, Paul Lorenz, Daniel Meldrim, Eric Motta, Alexander Pinho, Julia Porrino, Andrea Roeser, Fremy Santana, Chen Shu, Enkhsanaa Sommers, Sarp Uslu
Lab Instructor: Michael Lam; Instructor: Lou Kondic; Thanks to: Linda Cummings

Supported by NSF Grant No. DMS-1211713

Abstract

We present analytical, experimental, and numerical results for the Saffman–Taylor instability for a two-phase flow in a Hele-Shaw Cell. Experimentally, we have considered few different fluid combinations: water-glycerol and water-PEO (polyethylene oxide). PEO is a non-Newtonian fluid that exhibit more complex behavior such as shear thinning and elastic response. Theoretically, we have analyzed the stability of the simple (Newtonian) fluid interface and compared the predictions with the experimental results. Computationally, we have carried out Monte-Carlo type of simulations based on the so-called diffusion limited aggregation (DLA) approach. We have computed various measures of the emerging patterns, including fractal dimension for both experimental and computational results.

Experiment

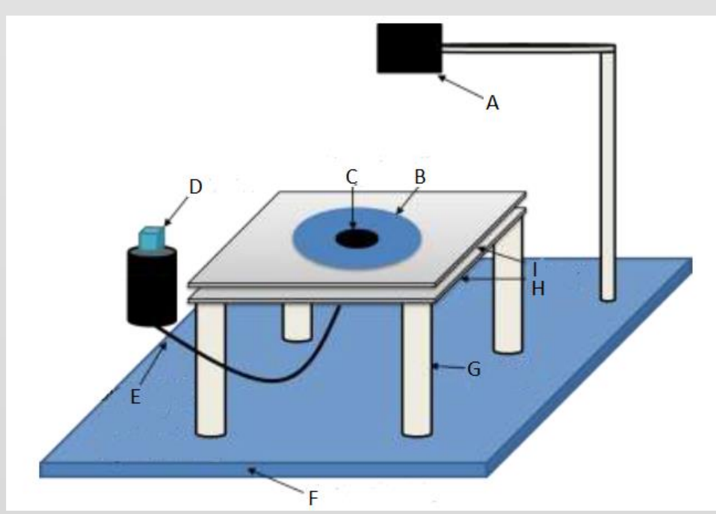

Setup/Procedure (see Figure 1):

Step 1 – 4 posts (G) are screwed into optical table (F) with wax paper background (H) resting on top

Step 2 - Various sizes of spacers are placed in between the plastic plates (I) for separation

Step 3 - The more viscous fluid (B) is poured on bottom plate and flattened out in between two plates (I)

Step 4 - Elevated syringe with tubing (E) to connect less viscous fluid (C) through a needle to a hole in the bottom plate

Step 5 - Various weights (D) placed on top of syringe

Step 6 - Simple smartphone video camera (A) placed on stand directly above cell

Parameters:

- Volume of injected water remains constant
- Cell spacing is kept constant at first, varying the weight placed on the syringe
- After various injection pressures, process is repeated for other cell spacings

Results:


Figure 2: 0.32mm spacing, Newtonian


Figure 3: 0.52mm spacing, Newtonian


Figure 4: 0.32mm spacing, Non-Newtonian


Figure 5: 0.52mm spacing, Non-Newtonian


Figure 6: 0.83mm spacing, Non-Newtonian

Linear Stability Analysis (LSA)

Stokes flow is a creeping flow whose transport force is smaller than the viscous force. Furthermore, the Reynolds number (a ratio of inertial to viscous forces) is small (Re<<1). A Hele-Shaw flow is a specific case of it, where the flow between two parallel plates that are spaced close to each other is considered. The Saffman–Taylor instability (viscous fingering) occurs when a less viscous fluid is forced into a more viscous fluid.

The model the instability, we consider the fluid-fluid interface to initially be circular with some small sinusoidal perturbation characterized by a wavenumber m. In addition, we include surface tension forces. At the injection point, we assume the flow satisfies Darcy's Law. Under these modeling considerations we derive the growth rate of the perturbations as a function of m. Assuming the mode, m, which maximize the growth rate is the mode that is observed, the number of observed fingers can be derived.

Darcy's Law:

$$u = -\frac{h^2}{12\mu}\nabla \mathrm{P}$$

Number of Fingers:

$$m = \sqrt{\frac{2\mu R_1 Q}{\pi h^3 \gamma} + \frac{1}{3}}$$

Where μ is the viscosity, R_1 is the average radius of the interface, Q is the injection flow rate, h is the cell spacing and γ is the surface tension. With the exception of flow rate, the other parameters are readily available. Experimentally only the amount of fluid and injection time are known. For simplicity Q is assumed to be constant in time.

Count Finger Number:

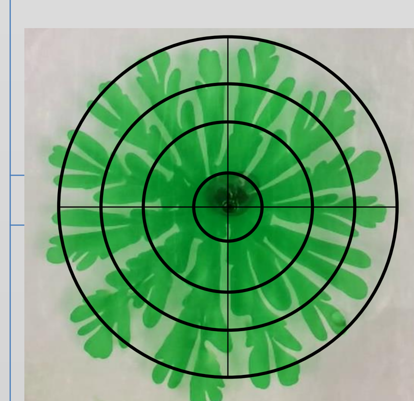

Measure vs. Theory

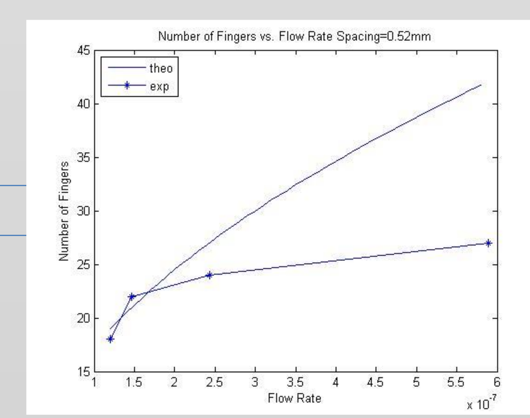

Diffusion Limited Aggregation

Diffusion limited aggregation is a numerical method based on the idea of Brownian motion. The random walkers begin walking from the outer edge of a circle whose center is the initial seed. The place the walker starts from is random and the movement the walker follows is also random— the walker moves north, south, east, or west until it reaches a previously stuck walker. The only thing a walker cannot do is leave the circle and if they attempt to do so, a new random movement is generated. As the aggregate of walkers grows larger, the circle expands to contain the entire aggregate.

Calculating of the sticking probability is based on the following method: sticking probability is linearly dependent on the number of occupied spaces around the current location (N_l), which is calculated by looking at a l by l matrix around the space the walker wants to stick (for our simulations we mainly kept l=9).

$$P_{newtonian} = A * \left(\frac{N_l}{l^2} - \frac{l-1}{2l}\right) + B$$

In Newtonian fluids the viscosity is constant. In the non-Newtonian case we use the idea that the shear rate depends on the fluid velocity. To simulate this effect, we adjust the sticking probability function such that the probability is higher around the recently occupied spaces. In order to implement this, one has to keep track of the order in which the particles stick to the aggregate and mark the unoccupied spaces around the interface by an order value. We refer to this value as the velocity number. In each addition to the cluster, the most recent stuck walker will be assigned a velocity number of one and the rest of velocity numbers will be incremented to preserve the order.

If the walker lands on the aggregate at a point where the velocity number is low, the probability of sticking is larger. Therefore, this local value at the point where the walker wants to stick appears in the denominator of the correction (see the probability function in the text that follows).

Furthermore, as the aggregate grows, the probability to stick on any spot on the interface gets smaller, simply because there are more spots to stick. All unoccupied spots, around the interface are approximately equal to the circumference of the cluster. However, calculating the circumference of a structure each time a particle attempts to stick with fractal properties is a difficult task. Therefore, we assume that the circumference is roughly equal to the square root of the cluster area. In other words, we assume the cluster is a circle for this calculation. This value appears in the numerator of the correction as shown below. Overall, we expect the correction to create the desired effect to simulate Non-Newtonian fluid flow.

$$P_{non-newtonian} = P_{newtonian} \times \left(1 + \frac{c \times currentClusterArea^{0.5}}{velocityNumberAtSite}\right)$$

$$clusterCircumference \approx clusterArea^{0.5}$$

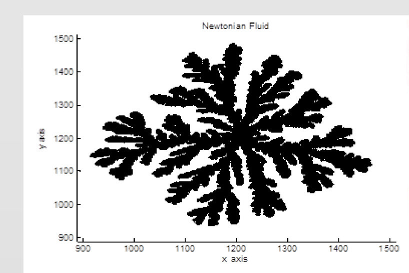

100,000 walkers, A = 3 and l = 9

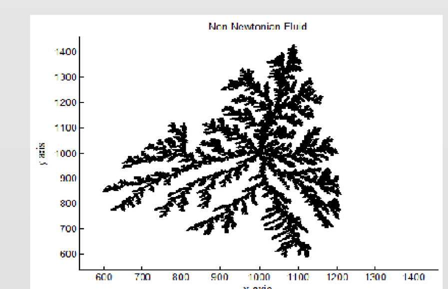

100,000 walkers, A = 1.5, C = 0.7, l = 9, and pp = 0.5

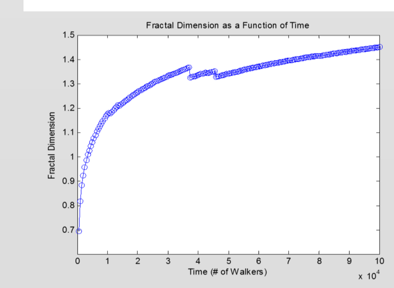

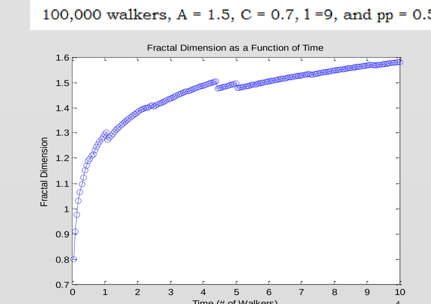

Boundary Integral Methods (BIM)

The idea of BIMs is that we can approximate the solution of a PDE by first finding the solution at the boundary. This is used primarily with large domains (both interior and exterior) where the finite difference method would require too many points for practicality.

We are looking for the solution $LP = 0$ where $L = \nabla^2$

A Green's function is any function that under the linear operator L follows $LG(x,y) = \delta(x-y)$. By the direct delta identities, we have

$$\int L\, G(x,y) f(y) dy = \int \delta(x-y) f(y) dy = f(x)$$

$L \int G(x,y) f(y) dy = LP$, implying that $\int G(x,y) f(y) dy = P(x)$

Green's identities show we can then represent the solution as

$$\int \frac{\partial G}{\partial n}(x,y) P(y) dy - \int G(x,y) \frac{\partial P}{\partial n}(y) dy = P(x)$$

It is common to write the integrals as operators

$$M\{P\} - L\{\mu\} = P$$

For BIM, we will either give P or $\mu = \frac{\partial P}{\partial n}$ on the boundary. BIM will be used to find the other.

The jump across the boundary $P_{in} - P_{out} = \tau\kappa$ and for an assumed constant pressure inside (for this experiment we used air), we have

$$P_{out}(x) = M\{P\} - L\{\mu\} = P_{in} - \tau\kappa$$

Discretizing the linear operator G(x,y), we can solve a system of linear equations to solve P & μ.

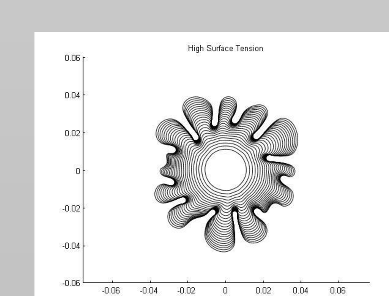

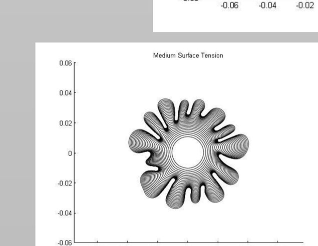

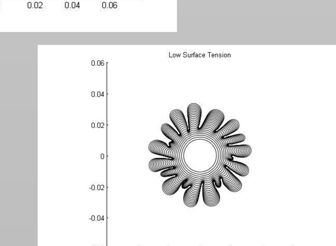

Application of Complex Variables

The movement of a fluid boundary within a Hele-Shaw cell can be modeled by the use of complex variables. With complex variables, a conformal map can be deduced within a zero surface tension (ZST) environment. A point from the **ζ**-plane can be mapped to the physical **z**-plane. This new domain will evolve over time.

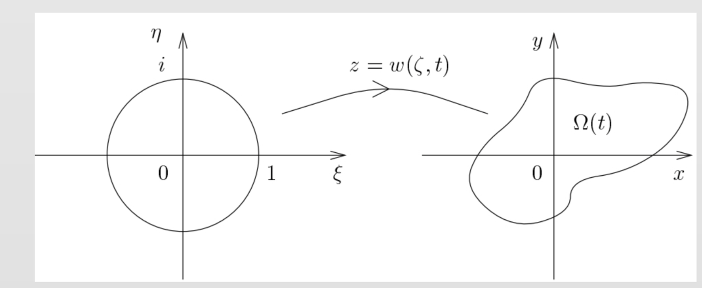

Figure 1; Free Boundary Models in Viscous Flow; Cummings, Linda.

The *Polubarinova-Galin* (P-G) equation can be derived by assuming the complex potential and the flow is driven by a single point sink of strength Q > 0. This results in the following:

$$R\left\{\zeta w'(\zeta) \overline{w}_t\left(\frac{1}{\zeta}\right)\right\} = -\frac{Q}{2\pi} \text{ with } |\zeta| = 1$$

Additionally, we have the Schwarz function, which is equivalent to the analytic continuation of the P-G equation, but much simpler in practice. Using a pre-defined function in tandem with a Laurent series about the suction point, we can solve the problem by equating coefficients from the expansions. A Schwarz function is defined by the equality:

$$g(z) \equiv \overline{w}\left(\frac{1}{\zeta}\right)$$

Using the P-G equation, we can generate a general quartic map.

$$z = w(\zeta, t) = a_1(t)\zeta + a_2(t)\zeta^2 + a_3(t)\zeta^3 + a_4(t)\zeta^4$$

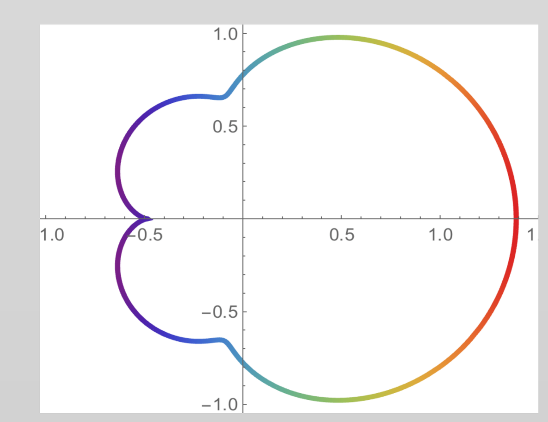

At a certain point in continuous time, the solution of the function becomes stiff (blow-up time). Once this happens, cusps form on the graph, which in turn causes the graph to begin to cross, and the solution becomes unstable.

Reference:

[1] Paterson, Lincoln. "Radial Fingering in a Hele Shaw Cell." *Journal of Fluid Mechanics* 113.-1 (1981): 513.
[2] Kondic, Lou (2014), Linear Stability Analysis of two phase Hele-Shaw Flow, Unpublished.
[3] Cummings, L.J. Free Boundary Models in Viscous Flow. Thesis (Ph.D.), University of Oxford (1996).
Davis, P.J. The Schwarz function and its applications. *Carus Math. Monographs* ***17**, Mathematics Association of America* (1974).
[4] Daccord, Gerard, Johann Nittmann, and H. E. Stanley. "Radial Viscous Fingers and Diffusion-Limited Aggregation: Fractal Dimension and Growth Sites." *Physical Review Letters* 56.4 (1986): 336-41.
[5] Kadanoff, Leo P. "Simulating Hydrodynamics: A Pedestrian Model." *Journal of Statistical Physics* 39.3 (1985): 267-83.
[6] Hadavinia, H, Fenner, R, & Advani, S 1995, 'The evolution of radial fingering in a Hele-Shaw cell using C1 continuous Overhauser boundary element method', Engineering Analysis with Boundary Elements, vol. 16, no. 2, p. 183-195.
[7] Kirkup, Stephen, and Javad Yazdani. *A Gentle Introduction to the Boundary Element Method in Matlab/Freemat*. *Boundary-Element-Method.com*. N.p., June 2008. 29 Mar. 2015.
[8] Cheng, H., W. Y. Crutchfield, M. Doery, and L. Greengard. "Fast, Accurate Integral Equation Methods for the Analysis of Photonic Crystal Fibers I: Theory." *Optics Express* 12.16 (2004): 3791.
[9] Davidson, M. R. "An Integral Equation for Immiscible Fluid Displacement in a Two-dimensional Porous Medium or Hele-Shaw Cell." *The Journal of the Australian Mathematical Society. Series B. Applied Mathematics* 26.01 (1984): 14.
[10] Hou, Thomas Y., John S. Lowengrub, and Michael J. Shelley. "Removing the Stiffness from Interfacial Flows with Surface Tension." *Journal of Computational Physics* 114.2 (1994): 312-38.
[11] Hou, T.y., J.s. Lowengrub, and M.j. Shelley. "Boundary Integral Methods for Multicomponent Fluids and Multiphase Materials." *Journal of Computational Physics* 169.2 (2001): 302-62.
[12] Kirkup, Stephen. *The Boundary Element Method in Acoustics: A Development in Fortran*. Hebden Bridge: Integrated Sound Software, 1998. Print.
[13] Laforce, Tara, and Ca 1St June 2006 Stanford. *PE281 Boundary Element Method Course Notes*.